Numerical investigation of the effect of nonlinear propagation distortion on helicopter noise

Penelope Menounou and Panagiotis Vitsas

University of Patras, Department of Mechanical and Aeronautical Engineering, Rion, 26504 Patras, Greece
menounou@mech.upatras.gr

Nonlinear propagation distortion causes energy to be shifted to the high frequency end of the spectrum. This leads to underestimation of the noise levels at high frequencies. The effect has been demonstrated in the case of aircraft noise, but less attention has been given to helicopter noise. In the present work, the effect of nonlinear propagation distortion on helicopter noise is presented based on measured data for low-speed descent and numerical calculations that predict the noise level away from the helicopter with and without nonlinear effects. It is shown that (i) for some frequency bands the difference between linear and nonlinear calculations can be as high as 8 dB, (ii) octave frequencies bands of 500, 1000 and 2000 Hz are more affected, and (iii) the effect is highly directional depending on the receiver location around the helicopter. It is further shown that nonlinear effects depend on the specific helicopter noise mechanism. More specifically, the following helicopter-specific noise source types are investigated with regards to nonlinear effects: advancing Blade Vortex Interaction (BVI) noise vs retreating BVI noise, High Speed Impulsive noise, and BVI vs Very Impulsive noise.

1   Introduction

Nonlinear propagation distortion effects manifest themselves when the noise signal is of sufficiently high intensity. Each part of the signal travels with its own velocity, namely the speed of sound plus the local velocity of the signal. Parts of the signal travel faster than the speed of sound, while others move slower. As a result, the original shape of the signal distorts and the frequency distribution of the signal changes accordingly. The effect has been studied in aircraft noise propagation, where is has been demonstrated that nonlinear effects are responsible for the higher values measured at high frequencies compared to the values predicted using linear propagation theory for the same frequencies [1,2,3].

Helicopter noise is quite different from aircraft noise. Firstly, it is of lower intensity than aircraft noise. The power spectrum has its maximum value in the lower frequencies and the noise signal itself is dominated by pulses, which are associated with the blade passages. In contrast, aircraft noise is of higher intensity, the power spectrum has its maximum value in the middle frequencies and the noise signal is more random. Finally, it should be added that helicopters produce a very directional noise field, while the field produced by aircraft is closer to that of an omni-directional source.

In the case of nonlinear propagation of helicopter noise, the literature is far less extensive and focuses in cases of transonic/supersonic flows around the blade tip, where shock waves are formed and after dislocating from the blade surface propagate in the surrounding medium [4] The purpose of the present work is (i) to demonstrate the effect of nonlinear propagation distortion for subsonic cases and (ii) to show the differences between the various types of noise signals produced by helicopters with regards to their nonlinear evolution.

2   Computational tool – Experimental database

As noise source we considered the sound pressure time-signals measured during the HELISHAPE project for low-speed descent [5]. The measurements were done with a four bladed rotor having a rectangular blade tip shape in the DNW windtunnel. The flight speed was 35 m/s, and the descent flight had a -6 deg path angle. Measurements were made at an array of 11 equally spaced microphones (see

Fig.1) with the array's span positioned normal to the flow (crossflow-y) and symmetrically arranged with respect to the rotor center (streamwise x). The noise signals measured at each such position on the grid were used as noise source signals coming from a directive stationary point source located at the rotor center and with source radius equal to the distance from the rotor center to the given microphone position. The measurements were conducted with a model rotor. For the purposes of the present work the measurements have been transformed into full scale motor using the scaling procedure of Ref 6.
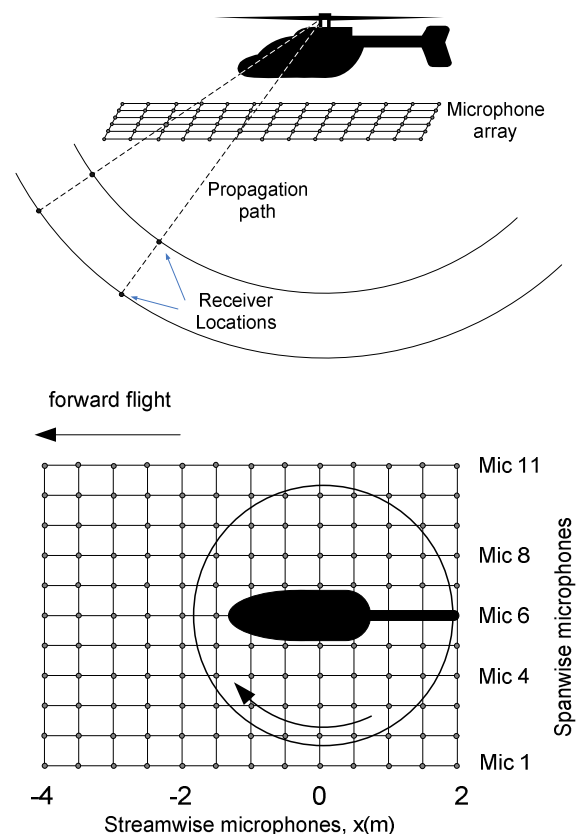
Fig.1 Geometry of the problem

The noise signals were propagated numerically distance R following the propagation path from the rotor head center through the microphone grid to receiver locations on the surface of a hemisphere as shown in Fig.1. The calculations have been performed twice, once including only linear propagation effects (geometrical spreading and atmospheric absorption) and a second time adding nonlinear propagation distortion to the linear calculations. The computations were performed in the time domain with the algorithm of Cleveland-Hamilton-Blackstock of Refs 7 and 8. The algorithm effectively solves the augmented Burgers

Equation with the split step method. The Burgers equation [9] is the simplest equation that combines the effects of nonlinearity and thermoviscous attenuation, which is augmented to take into account spherical spreading and relaxation effects of O_2 and N_2 in the atmosphere.

The nonlinear propagation distortion effects after propagation distance R are presented as the difference in the SPL value with and without nonlinear propagation distortion effects at each one-third octave band:

$$DSPL(f;R) = SPL_{nonlinear}(f;R) - SPL_{linear}(f;R) \quad (1)$$

The resulted DSPL vs frequency plots for various propagation distances are shown throughout the paper. DSPL can, in some cases, be as high as 8 dB. This difference is of the same order as the effect of atmospheric absorption over the same propagation distance. Nonlinear distortion being an accumulative effect increases with distance. Results are shown up to 1000 m of propagation distance. For longer distances the higher frequencies first and the lower frequencies later attenuate completely until the signal ceases to be heard.

3 Helicopter specific noise

Helicopters produce a complicated, highly directional noise field, where considerably different noise signals at various points around the helicopter are attributed to different noise generation mechanisms. In the following the qualitative behaviour of these helicopter specific noise signals is presented with regards to their nonlinear propagation distortion. Specifically, we shall examine (i) Blade Vortex Interaction noise (BVI) in the advancing side of the flow field as compared with BVI noise in the retreating side, (ii) BVI noise in the advancing side compared to Very Impulsive noise Signals (VIS) also in the advancing side, and (iii) High Speed Impulsive Noise (HSI) with and without the presence of shocks .

3.1 Advancing side / retreating side blade vortex interaction noise

Helicopters produce a highly directional field and accordingly nonlinear distortion effects (expressed in DSPL) depend highly on the receiver location. The most marked difference is observed between advancing and retreating side. Fig.2 shows a typical advancing side BVI signal (measured at mic3 / x=0) and a typical retreating side BVI signal (measured at mic11 / x=2). The prediction of their evolution with and without nonlinear propagation effects yields the DPSL shown also in the Figure. It can be observed that the two cases differ markedly in both the amplitude and the sign of DSPL. In the former, the difference between linear and nonlinear calculations is 4 dB and predominantly positive, while in the latter is approximately 1 dB and predominantly negative. The DSPL plot in the advancing side assumes, unlike in the retreating side, the characteristic shape of a bell, which will be called *DSPL bell* hereinafter.

The difference in the behaviour between advancing and retreating side BVI can be explained by observing the

evolution of the main pulses, which have been isolated from the two signals (see Fig.3). In order to clearly show the effect, only nonlinear distortion was considered. Geometrical spreading and atmospheric absorption effects were ignored, thus, effectively considering the case of plane wave propagation in a non-dissipative fluid. It can be observed that the segment of the signal connecting the peak with the trough steepens due to nonlinear propagation in the advancing side, while it un-steepens in the retreating side. In the frequency domain, accordingly, energy is transferred from the middle frequencies towards higher frequencies in the advancing side, while in the retreating side energy is still transferred from the middle frequencies to higher frequencies, but towards lower frequencies as well.
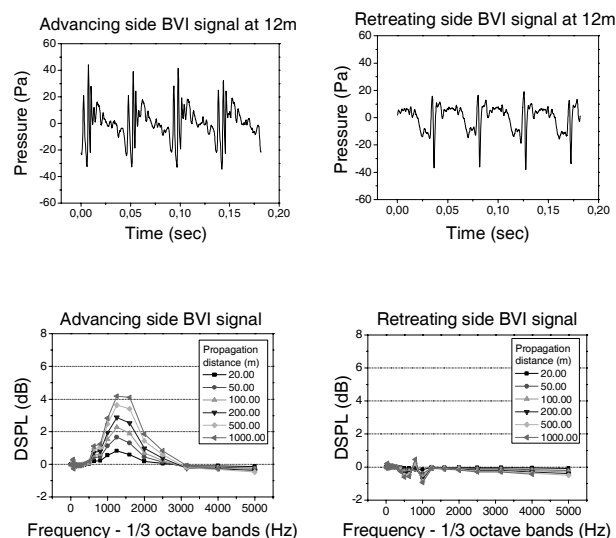
Fig.2 Advancing and retreating side BVI signals and the nonlinear propagation distortion of their spectra.
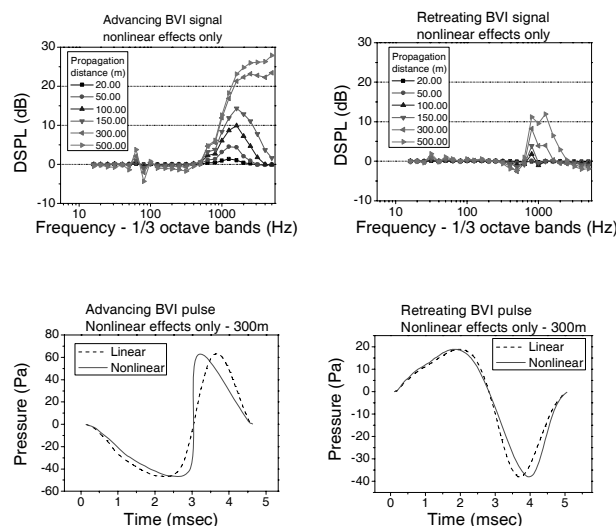
Fig.3 Nonlinear propagation distortion of advancing and retreating side BVI signals and their corresponding spectra (geometrical spreading and atmospheric absorption ignored).

All measured signals evolve either as an advancing side type signal, yielding the characteristic DSPL bell, or as a retreating side type signal. The following differences between them are common in all receiver locations: (i) the DSPL values in the advancing side are substantially larger than in the retreating side, (ii) the DSLP values are predominantly positive in the advancing side, while predominantly negative in the retreating side, (iii) the frequencies mainly affected in the advancing side are the frequencies in the octave bands of 1000 Hz and 2000 Hz, while the frequencies mainly affected in the retreating side are frequencies from 300 Hz to 1000 Hz, and (iv) although very small in magnitude, DSPL in the lowest frequency bands, up to 300 Hz, are negative in the advancing side, while positive in the retreating side.

A new quantity has been derived that provides an indicator of the tendency of the signal to "steepen" and thus follow an advancing side type nonlinear evolution or "un-steepen" and thus follow a retreating side type nonlinear evolution. The quantity is termed *polarity* and it is based on the observation that the middle signal in Fig.4 describes advancing side type signals and the right signal in Fig.4 describes retreating side type signals. The former is assigned a positive polarity, the latter negative and the left signal in Fig.4 has zero polarity. Polarity is computed as follows:

$$\Pi^3 = \frac{\sum_{i=2}^{N} P_{i-1}^{+}\left(\Delta P_i^{+}\right)^2}{N^{+}} - \frac{\sum_{i=2}^{N} P_{i-1}^{-}\left(\Delta P_i^{-}\right)^2}{N^{-}} \qquad (2)$$

where N is the number of points in the waveform, P_i is the value of the pressure at point i, $\Delta P_i = P_i - P_{i-1}$, P^+ is the pressure at point i, when $\Delta P_i > 0$, P^- is the pressure at point i when $\Delta P_i < 0$, N^+ is the number of points for which $\Delta P_i > 0$, and N^- is the number of points for which $\Delta P_i < 0$.

Fig.4 Idealized pulses with zero (l), positive (m), and negative (r) polarity.

It should be emphasized that the same quantity can also be used to characterize signals with mixed advancing and retreating side characteristics as either advancing or retreating. Figure Fig.5 shows the polarity of all measured signals, where it can be observed that the sign of the polarity on a plane below the helicopter coincides with the traditional advancing and retreating side BVI regions at descent flight [10]. As far as nonlinear distortion is concerned, signals with negative polarity exhibit a retreating side type DSPL, while signals with positive polarity the characteristic DSPL bell.
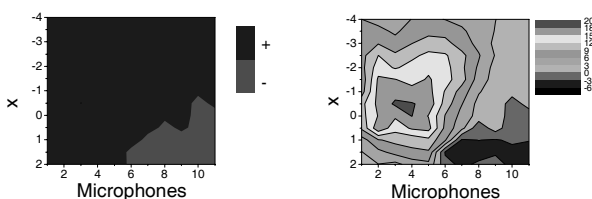
Fig.5 Contour plot of the polarity of the noise source signals. Negative polarity corresponds to retreating side

type nonlinear distortion evolution. Positive polarity corresponds to advancing side type nonlinear distortion evolution.

3.2 Advancing side blade vortex interaction noise – very impulsive noise

Noise signals on the upstream side, depending on the receiver location around the helicopter, vary considerably in shape ranging from BVI signals with multiple peaks at each blade passage to single peak very impulsive signals (VIS) at each blade passage. Figure 6 shows an example of four measured signals where the above mentioned transition can be observed from signals A to D. The prediction of their evolution with and without nonlinear propagation effects yields the DPSL bells shown next to each noise signals. It can be observed that the DSPL bell moves to higher frequencies as the signal transitions from multiple peaks BVI to VIS.
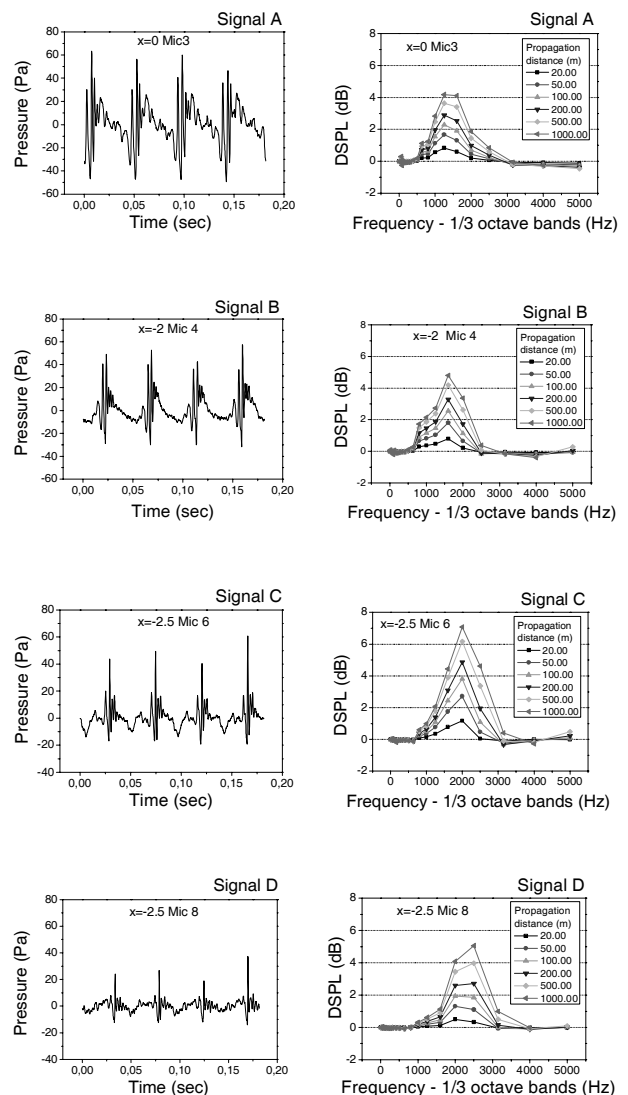
.Fig.6 As the pressure signal at source transitions from containing multiple BVI peaks to single pulse of short duration, their corresponding DSPL bells move to higher frequencies.

Numerical experimentation performed by changing various characteristics of the noise source signals and predicting

anew the DSPL bell of the altered signals showed that: (i) the starting frequency f_{start} of the DSPL bell (that is the lowest 1/3 octave frequency band affected by nonlinear distortion) depends on the rise time, and (ii) the ending frequency f_{end} of the DSLP (that is the highest 1/3 octave frequency band exhibiting a positive DSPL value) depends on the curviness of the main pulse's peak. *Rise time*, Δt, is the time between the peak and the trough in the main pulse of the BVI signal. *Curviness*, K, is a measure of how curved is the (positive) peak of the signal's main pulse and is computed as follows:

$$K = \sum_{i=i_{max}-1}^{i_{max}+1} (P_i - 2P_{i-1} - P_{i-2}) \qquad (3)$$

where i_{max} is the point of the waveform at which the pressure signal's main pulse has its peak. Rise time is associated with the first derivative of the pressure, while curviness with the second derivative.

An examination of f_{start} and f_{end} on all measured signals in the area that exhibits advancing side type nonlinear behavior showed that: (i) f_{start} occurs at one of the following 1/3 octave frequency bands 800, 1000, 1250 Hz, (ii) the bell moves to lower frequencies for larger values of rise time and to higher frequencies for smaller rise time (see Fig. 7), (iii) the ending frequency of the DSPL bell in most cases occurs at the 2000 Hz and 2500 Hz 1/3 octave frequency bands, and (iv) f_{end} moves to higher frequencies for larger absolute values of the curviness (sharper peaks) and to lower frequencies for smaller values of curviness (more curved pulses).
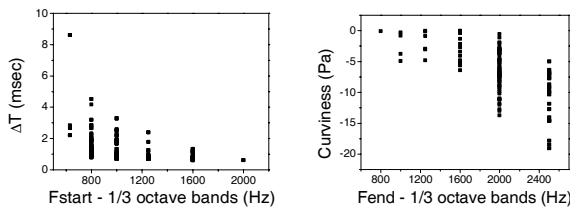
Fig. 7 Effect of rise time (Δt) on f_{start} and of curviness (K) on f_{end} .

Figure Fig.8 (a) shows that noise source signals in upstream locations have pulses of shorter durations than noise signals in downstream locations. Consequently, f_{start} occurs at higher 1/3 octave bands in the upstream locations than it does in the downstream locations (see Fig.8). Figure Fig.8(b) also shows that noise signals on upstream locations in the retreating side have the sharpest peaks (smallest values of K). Consequently, f_{end} occurs at higher 1/3 octave frequency bands in the upstream locations of the retreating side (see Fig.8).
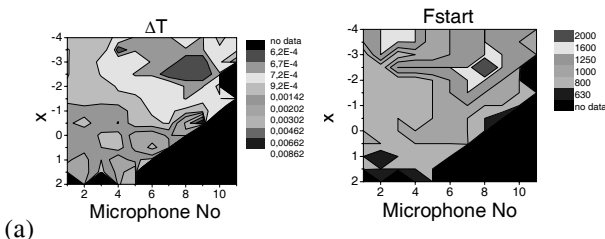
(a)
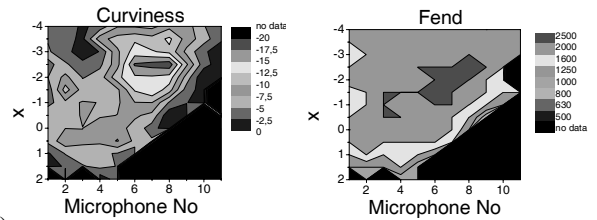
(b)

Fig.8 Contour plots of f_{start}, f_{end}, rise time (Δt), and curviness (K) on all measured signals that exhibit an advancing side type nonlinear evolution.

3.3 High speed impulsive noise

High speed impulsive noise is a case of particular interest, as the amplitude of the pressure obtains large values (much larger than in BVI noise). Figure Fig.9 shows two cases of HSI noise, both for lifting forward flight, one below a four-bladed rotor with advancing tip Mach number 0.881 (shown on the left column) taken from ref [11], and one on the rotor plane of a two-bladed rotor with advancing tip Mach number 0.931 (shown on the right column) taken from ref [12]. In the former the advancing tip Mach number is below the delocalization Mach number and the signal contains pulses with large gradient, but no shocks, while in the later the advancing tip Mach number is above the delocalization Mach number and the signal contains shocks.
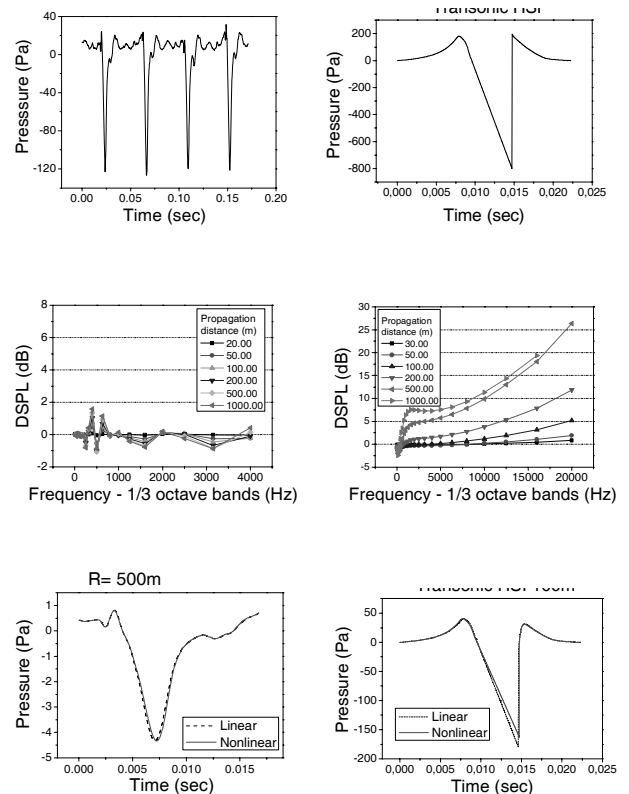
Fig.9 Two case of HSI noise, (l) advancing tip Mach number 0.881, (r) with advancing tip Mach number 0.931.

Fig.9 also shows the resulting nonlinear evolution of the signals as DSPL plots. It can be observed that when shocks are present in the signal, DSPL resembles more to the DSPL of aircraft noise, where nonlinear effects are amplified with frequency. It should also be noted that the

values of DSPL are considerably larger than in the BVI case. For the shock-free HSI case, the nonlinear evolution is quite different and with smaller DSPL values compared to the HSI with shocks. Finally, it should be observed that below the delocalization Mach number the nonlinear behavior is a retreating side type, while above the delocalization Mach number an advancing side type. It should be mentioned that, as expected, in the former case the noise source signal has negative polarity and in the later positive polarity.

4   Conclusion

In the present work, the effect of nonlinear propagation distortion on helicopter main rotor noise was presented based on measured data for low-speed descent and numerical calculations based on the augmented Burgers equation that predict the noise level away from the helicopter with and without nonlinear effects. It was shown that (i) for some frequency bands the difference between linear and nonlinear calculations can be as high as 8 dB, (ii) the octave frequency bands of 500, 1000 and 2000 Hz are more affected, and (iii) the effect is highly directional depending on the receiver location around the helicopter. Furthermore, nonlinear propagation effects were categorized depending on the type of the noise signal. Two main types of nonlinear evolution were distinguished, advancing side type and retreating side type. A new quantity, termed polarity was derived to characterize a noise source signal as advancing or retreating side type in terms of its nonlinear evolution. Advancing side type evolution was further examined and categorized based on time signal's characteristics. Finally, high speed impulsive noise signals (with and without shocks) were considered and evaluated with regard to their nonlinear propagation distortion.

Acknowledgments

References

[1] S. McInerny, K. L. Gee, M. Dowing, M. James, "Acoustical Nonlinearities in Aircraft Flyover Data," *AIAA* Paper 2007-3654 (2007)

[2] H. H. Brouwer, "Numerical Simulation of Nonlinear Jet Noise Propagation," *AIAA* Paper 2005-3088 (2005)

[3] K. L. Gee, V. W. Sparrow, T. B. Gabrielson, A. A. Atchley, "Nonlinear Modeling of F/A-18E Noise Propagation," *AIAA* paper 2005-3089 (2005)

[4] Barger, R. L. Theoretical prediction of nonlinear propagation effects on noise signatures generated by subsonic or supersonic propeller or rotor-blade tips. May 1, 1980. NASA-TP-1660; L-13388.

[5] K.-J Schultz, W. Splettstoesser, B. Junker, W. Wagner, E. Schoell, E. Mercker, K. Pengel, G. Arnaud, D. Fertis,"A parameteric windtunnel test on rotorcraft aerodynamics and aseroacoustics (Helishape) – test procedures and representative results," 22nd European Rotorcraft Forum, Brighton, UK, 1996

[6] Schmitz F H: Rotor noise. NASA Ames Research Center, Moffett Field, California, 1991

[7] R. O. Cleveland, M. F. Hamilton, D. T. Blackstock, "Time-domain modeling of finite-amplitude sound in relaxing fluids," *J. Acoust. Soc. Am.* 99, 3312-3318 (1996)

[8] Y.-S. Lee, M. F. Hamilton, "Time-domain modeling of pulsed finite-amplitude sound beams," *J. Acoust. Soc. Am.* 97, 906-917 (1995)

[9] Nonlinear Acoustics, edited M.F.Hamilton and D.T.Blacktock, Academic press, 1998

[10] Splettstoesser WR, Kube R, Wagner W, Seelhorst U, Boutier A, Micheli F, Mercker E, Pengel K. Key results from a higher harmonic control aeroacoustic rotor test (HART). J American Helicopter Society 1997;42(1)

[11] A. S. Morgans, S. A. Karabasov, A. P. Dowling, and T. P. Hynes. Transonic Helicopter Noise. AIAA Journal Vol. 43, No. 7, July 2005

[12] Schmitz F.H., Boxwell D.A., Splettstoesser W.R. and Schultz K.J. Model-rotor high speed impulsive noise: Full-scale comparisons and parametric variations, Vertica Vol. 8, No. 4, pp. 395-442, 1984